VOL. 18, NO. 5, MARCH 2023 ISSN 1819-6608
ARPN Journal of Engineering and Applied Sciences

www.arpnjournals.com

SYNTHESIS OF REDUCED GRAPHENE OXIDE FROM OIL PALM EMPTY FRUIT BUNCHES USING MATOA LEAF EXTRACT

Muhammad Said[1], Nadia Lestari[1], Maria Ulfa[1], Addy Rachmat[1], Desnelli[1] and Muhammad Faizal[2]
[1]Department of Chemistry, Faculty of Mathematics and Natural Sciences, Sriwijaya University, Jalan Palembang-Prabumulih, Indralaya, Indonesia
[2]Department of Chemical Engineering, Faculty of Engineering, Sriwijaya University, Jalan Palembang-Prabumulih, Indralaya, Indonesia
E-Mail: msaidusman@unsri.ac.id

ABSTRACT

Reduced graphene oxide is a compound produced by removing oxygen-containing functional groups from graphene oxide. It was synthesized from oil palm empty fruit bunches because of their abundance and carbon elements to obtain an efficient adsorbent. Furthermore, the synthesis was conducted by using the Hummer method, and graphene oxide was reduced by matoa leaf extract. Characterization analysis with XRD reported an angle 2θ peak of 24.4º with a d-spacing value of 0.365 nm, while FTIR showed the O–H, C≡N, C=C, and C–H functional groups with lower intensities than GO. Characterization by Raman spectroscopy reported a D peak at 1381 cm^{-1}, G at 1592 cm^{-1}, and 2D at 2685 cm^{-1} with a defect intensity ratio compared to the graphite of 0.93. Meanwhile, the synthesized reduced graphene oxide was applied as an adsorbent to adsorb methylene blue. The concentration of the adsorbent showed the optimum conditions for the adsorption of methylene blue at the optimum concentration of 50 mg/L, the optimum time of 45 minutes, and the optimum adsorbent mass of 25 mg for 36.95 mg/L, 42.40 mg/L, and 49.856 mg/L, respectively. The reduced graphene oxide adsorption isotherm followed the Langmuir model with a correlation coefficient, maximum adsorption capacity, and a K_L value of 0.9998, 54.945 mg/g, and 0.587 L/mg.

Keywords: OPEFB, reduced graphene oxide, hummer, methylene blue, adsorption.

INTRODUCTION

Rapid technological developments require higher support for superior materials in applying sensors, adsorbents, catalysts, and capacitors. One of the materials being developed is graphene. Novoselov *et al.* (2004) stated that the compound is a two-dimensional monatomic material consisting of a single layer of graphite. The attractive characteristics of graphene, such as high mechanical strength, are caused by the regular arrangement of carbon atoms whose structure resembles a honeycomb (Smith *et al*., 2019) with a hexagonal skeleton and allotropy of carbon in the outermost layer (Magne *et al*., 2021). Graphene oxide (GO) is a derivative of a carbon layer composed of many oxygen functional groups (Jirickova *et al*., 2022).

Many methods can carry out the process of exfoliating graphite into GO. Some techniques used are chemical vapor deposition, ultrasonication, and Hummer. Products produced through chemical vapor deposition have high purity but require high production costs (Hashmi *et al*., 2022). Furthermore, the ultrasonication method uses ultrasonic waves to exfoliate the graphite layer (Yang *et al*., 2022) but produces GO with low purity and causes noise during production. Hummer uses chemical compounds to exfoliate graphite and is easy to carry out, efficient, and relatively inexpensive, but produces toxic waste and low GO purity (Chasanah *et al*., 2021). The Hummer method can produce graphene oxide on a large scale and is more effective when followed by a reduction process (Hessain and Hassan, 2019). The removal of some oxygen functional groups with reducing agents will produce reduced graphene oxide (Razaq *et al.,* 2022). Properties similar to graphene and low production costs have led to the development of research on the synthesis of graphene oxide. Grace and Malar (2020) used biomass in the form of coconut fiber to synthesize graphene oxide from ash. Research conducted through a test with XRD showed the presence of the oxide bands at an angle 2θ of 10.13º.

Oil palm empty fruit bunches (OPEFB) also have potential raw materials for synthesizing the oxide from coconut shells. The analysis of OPEFB shows the number of components, including 50.9% cellulose, 29.6% hemicellulose, and 17.84% lignin (Padzil *et al*., 2020). These components are composed of several carbons, namely 40.93 to 68.3% in one bunch used as carbon sources (Thoe *et al*., 2019). Oil palm is an essential commodity in Indonesia, the largest oil-exporting country in the world (Wdiatmoko *et al*., 2019). The plantation area reached 11.26 million Ha in 2015 and increased to 12.31 million Ha in 2017, with a total production of 31.07 million tons (Rahayu *et al*., 2021). This is in line with the abundant availability of OPEFB, but the utilization is not maximized (Sari *et al*., 2021). Research innovation on OPEFB needs to be carried out to produce more valuable compounds. It is used as an adsorbent obtained through synthesizing oil palm empty fruit bunches of charcoal into reduced graphene oxide.

The rGO in this research is applied as a methylene blue adsorbent. As a cationic dye, methylene blue is widely used in the cotton and paper coating industries (Suma *et al*., 2021). It has become one of the industrial wastes in water that cause environmental problems (Teow *et al*., 2021). Furthermore, adsorption is the most commonly used method to remove methylene blue content from the water. This method is widely used because it is relatively inexpensive, simple, and easy to be implemented (Khan, 2020).

Previous research on the application of reduced graphene oxide from OPEFB as methylene blue adsorbent was conducted by Rebitanim *et al.* (2012), with a maximum adsorption capacity (Q_m) at the Langmuir isotherm of 50.76 mg/g. OPEFB was synthesized into reduced graphene oxide by modifying the reducing agent in the form of matoa leaf extract.

Based on the above considerations, this research was conducted to obtain an efficient adsorbent in adsorption capacity. Several steps conducted in sample preparation were carbonization of OPEFB, graphitization, synthesis of graphene oxide, and reduction of graphene oxide using matoa leaf extract. The characterization was carried out using X-Ray Diffraction (XRD), Fourier Transform Infra-Red (FTIR), and Raman spectrophotometer. Furthermore, the application of rGO as an adsorbent was performed using the batch method under various conditions, such as concentration, contact time, and adsorbent mass. The residual methylene blue was analyzed using a UV-Vis spectrophotometer.

MATERIALS AND METHODS

Materials

The materials used were deionized water, distilled water, hydrochloric acid (HCl), 98.9% sulfuric acid (H_2SO_4) *Merck*, matoa leaves, ice cubes, iron (III) chloride hexahydrate ($FeCl_3{\cdot}6H_2O$) *Merck*, ethanol (C_2H_5OH), hydrogen peroxide (H_2O_2), potassium permanganate ($KMnO_4$) *Merck*, methylene blue, sodium nitrate ($NaNO_3$), and oil palm empty fruit bunches.

PROCEDURES

Carbonization of Oil Palm Empty Fruit Bunches

OPEFB was crushed, and the sample pieces of the same size were separated. The samples were washed thoroughly with water and dried for 5 days using sunlight. Furthermore, they were wrapped in aluminium foil and put in a ceramic dish. The samples were oven-dried at 100ºC for 60 minutes and put into the furnace at 600ºC for 180 minutes with the heating rate method at 5ºC/minute. The OPEFB charcoal was ground and sieved with a 200 mesh vibrator screen to form graphite(Akhavan *et al.*, 2014). The charcoal obtained was characterized using XRD.

Graphitization of Carbonization Results

The carbonization resulted in 1 g of charcoal powder and 0.5 g of $FeCl_3{\cdot}6H_2O$ being put in a 250 mL beaker, then 100 mL of deionized water was added, and the mixture was homogenized. The degree of acidity was adjusted by adding HCl and stirring at 500 rpm using a magnetic stirrer at 60°C for 5 hours. The mixture was left for one week to obtain optimal results. Furthermore, the mixture was filtered using a set vacuum apparatus, and the residue was dried in an oven at 100°C for 5 hours to form a black solid. Graphite was ground with a mortar (Akhavan *et al.*, 2014) and characterized using XRD and FTIR.

Synthesis of Graphene Oxide

The graphitization resulted in 1 g of graphite powder based on activated carbon from oil palm empty fruit bunches being put into a 250 mL beaker. Furthermore, it was placed in a container containing ice cubes with 50 mL of H_2SO_4 (98.9%) and stirred at 500 rpm using a magnetic stirrer at 80ºC for 24 hours. About 1 g of $NaNO_3$ was added to the solution and stirred in a container of ice cubes placed in a water bath for one hour before adding 6 g of $KMnO_4$ and stirring continuously for 4 hours.

The solution was heated in a water bath with a temperature of 35ºC for one hour and continued with the addition of 100 mL of distilled water by keeping the temperature below 60ºC. After 15 minutes, it was added with 6 mL of H_2O_2, diluted with 200 mL of distilled water, and centrifuged 10 times at 8000 rpm (30 minutes). Filtration was conducted two to five times while washing with deionized water to obtain a graphene oxide precipitate.

The results were added with deionized water to obtain a yellow-brown suspension. The solution was centrifuged at 2000 and 8000 rpm for 30 and 60 minutes. The suspension was ultrasonicated for 30 minutes, and the mixture was filtered using a set of vacuum apparatus to remove the residue and dried for 5 hours at 60º in an oven(Akhavan *et al.*, 2014). The synthesis results were characterized using XRD and FTIR.

Preparation of Reducing Agent from Matoa Leaves

The matoa leaves were first cleaned with tap water and washed with deionized water 2-3 times. The leaves were dried in an oven at a temperature of 50°C for 5 hours or left overnight and ground in a blender to a powder. Furthermore, 5 g of leaf powder was put into a boiling flask and added with 50 mL of deionized water. The mixture was refluxed for 1 hour at 80°C, and after cooling, the extract was filtered to obtain the filtrate (Parthipan *et al.*, 2021).

Reduction of Graphene Oxide

Reduced graphene oxide was prepared by adding one gram of GO with 25 mL of deionized water and 25 mL of matoa leaf extract. Furthermore, the mixture was ultrasonicated for 40 minutes and was put into a sterile Teflon-coated autoclave and oven at 100°C for 12 hours. The mixture was centrifuged at 8000 rpm for 15 minutes, and rGO was separated and washed with deionized water and absolute ethanol. The mixture was filtered using a vacuum to remove the residue and the oven at 60°C for 12 hours (Parthipan *et al.*, 2021). The synthesis results were characterized using XRD, FTIR, and Raman spectrophotometer.

Determination of Methylene Blue Standard Curve

First, 1000 mg/L mother solution from 0.5 grams MB was prepared for the standard solution with concentrations of 1, 2, 3, 4, and 5 mg/L through multilevel dilutions. The 50 mg/L MB solution was determined for the maximum wavelength using a UV-Vis spectrophotometer in the 650-670 nm range to obtain 664

nm. Subsequently, the absorbance of the standard solution was determined, and a curve was made.

METHYLENE BLUE ADSORPTION

Test with Variation of Concentration

About 10 mg of the sample was added to 15 mL of methylene blue with concentrations of 30, 40, 50, 60, and 70 ppm. The mixture was stirred using a stirrer at 200 rpm for 30 minutes, and a fixed volume of the dye solution was taken after the interval and centrifuged at 2000 rpm. Furthermore, the absorbance was measured using a UV-Vis spectrophotometer at the maximum wavelength of methylene blue.

Test with Variation of Contact Time

Approximately 10 mg of the sample was added to 15 mL of methylene blue with the optimum concentration obtained from the previous procedure. The mixture was stirred with a stirrer for 15, 30, 45, 60, and 75 minutes. A fixed volume of the dye solution was taken after the interval and centrifuged at 2000 rpm. Subsequently, the absorbance was measured with a UV-Vis spectrophotometer at the maximum wavelength of methylene blue.

Test with variation of adsorbent mass

About 5, 10, 15, 20, and 25 mg of each sample were added to 15 mL of methylene blue with the optimum concentration and time obtained from the previous procedure. The mixture was stirred at 200 rpm for 30 minutes. A fixed volume of the dye solution was taken after the interval and centrifuged at 2000 rpm. Furthermore, the absorbance was measured with a UV-Vis spectrophotometer at the maximum wavelength of methylene blue.

Data Analysis

Data analysis was conducted on the synthesis through sample characterization and its application in adsorption. The application procedure in the form of methylene blue adsorption aimed to determine the ability of the results to adsorb dye. The value of adsorption capacity and isotherm can be calculated using the following equation.

Adsorption Capacity

$$Q_e = \frac{(C_0 - C_e)\,x\,V}{W} \quad \text{.....(1)}$$

Langmuir adsorption isotherm:

$$\frac{C_e}{Q_e} = \frac{1}{Q_m K_L} + \frac{C_e}{Q_m} \quad \text{.....(2)}$$

Freundlich adsorption isotherm:

$$\log Q_m = \log K_F + \frac{1}{n}\log C_e \quad \text{.....(3)}$$

Description

Q_e = adsorption capacity at equilibrium (mg/g)
C_o = dye concentration (mg/L)
C_e = dye concentration at equilibrium (mg/L)
V = volume of dye solution (L)
W = adsorbent mass (g)
Q_m = maximum adsorption capacity (mg/g)
K_L = Langmuir isotherm constant
K_F = Freundlich isotherm constant
n = adsorption intensity

RESULTS AND DISCUSSIONS

Characterization of Synthesis Results

Data analysis results with XRD

XRD is used to investigate the crystal phase and determine the distance between layers or the d-spacing value (Hidayah *et al*., 2017), and the analysis is based on the position of angle 2θ. The diffractogram obtained through the XRD test is shown in Figure-1.

Figure-1 shows the diffraction pattern at angle 2θ, almost the same but with a different absorption intensity. Figure-1(a) shows a wide (amorphous) charcoal powder pattern, while the graphite in Figure-1(b) increases in intensity towards the crystalline phase with a not-too-sharp peak indicating that the graphitization process is not complete. Furthermore, Figure 1(c) shows the amorphous GO diffraction pattern. The rGO pattern is also amorphous, but the intensity decreases. This is in line with Joshi *et al*. (2020), who show sharp peaks in graphite while rGO is amorphous.

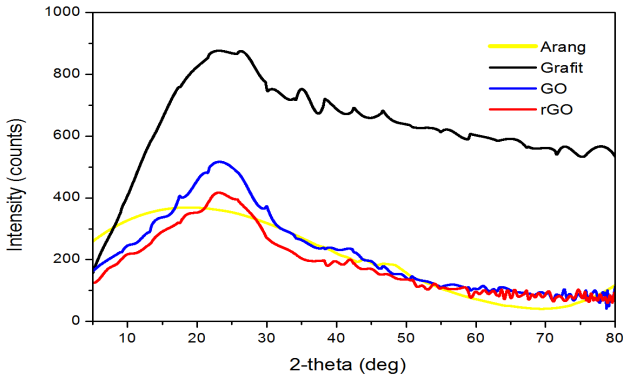

Figure-1. Diffractogram of XRD analysis results on charcoal powder (a), graphite (b), GO (c), and rGO (d).

The detail data from XRD is listed in Table-1.

Table-1. XRD Data on graphite, GO, and rGO.

Sample	2θ (°)	d-spacing	Intensity (cps)
Graphite	26.7	0.334	878.5
GO	23.3	0.381	516.9
rGO	24.4	0.365	418.9

Table-1 shows that graphite is located at an angle 2θ of 26.7º, indicating a well-arranged layer structure with a d-spacing value of 0.334. The 2θ peak formed is not too sharp because the graphitization process is imperfect and GO shows a shift in the 2θ peak to 23.3º. The distance between layers increases to 0.381 due to binding oxygen functional groups to the carbon base plane.

Hidayah *et al*. (2017) showed a shift in the 2θ peak of GO to 9.03º with a d-spacing value of 0.9794. The angle 2θ shift is not significant hence the oxidation has not taken place completely. The oxygen functional group is removed by reduction, while the 2θ peak and d-spacing become 24.4º, and 0.3648. The arrangement is not good when the rGO only covers one or several layers (Hidayah *et al.,* 2017).

Data analysis results with FTIR

Characterization with FTIR aims to compare the functional groups in GO and rGO. Each functional group has a different wavenumber due to differences in the ability to vibrate and absorb energy. The spectrum formed is shown in Figure-2.

Based on the spectrum in Figure 2, the absorption variation of rGO is very close to GO. Functional group analysis is conducted by looking at the spectrum peak. Figure-2(a) shows the GO spectrum, while rGO is shown in Figure-2(b). The analysis is based on the decrease in intensity of rGO, as shown in Table-2, and the loss of oxygen functional groups.

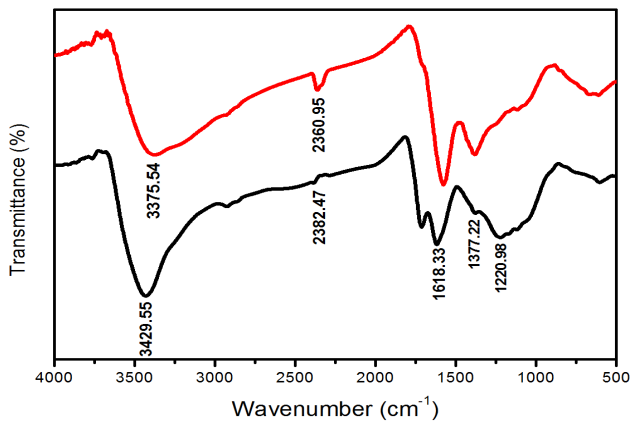

Figure-2. Spectrum of analysis results with FTIR on GO (a) and rGO (b).

Prediction of functional groups derived from OPEFB includes O–H (3600-3200 cm^{-1}), indicating the presence of hydroxy compounds in hemicellulose, cellulose, and lignin that are not completely carbonized or the presence of water added during the synthesis stage. The CN group (2400-2300 cm^{-1}), C=C (1650-1550 cm^{-1}), and C–H (1432-1319 cm^{-1}) indicates nitrile, alkene, and the vibrating CH2 in the aromatic polysaccharide (Thoe *et al*., 2019).

In addition, the complete data is listed in Table-2.

Table-2. FTIR Spectrum data.

GO		rGO	
Wavenumber	**Intensity**	**Wavenumber**	**Intensity**
3429,55	73,808	3375,54	72,792
2382,47	87,660	2360,95	84,352
1618,33	79,553	1577,82	68,905
1377,22	83,670	1381,08	73,865

Based on Table-2, the data analysis does not show any loss of oxygen-containing functional groups in the rGO spectrum, hence the reduction was not successful. The ratio of matoa leaves causes the failure of the process and the flavonoid compounds are still very small. Neutrally, charged extracts complicate the GO reduction procedure.

Data analysis results with raman spectrum

Raman spectroscopy is used to identify the occurrence of structural defects in the material (Jagiello *et al*., 2020) and the sample used is rGO. Identification is based on the D, G, and 2D bands indicated by the spectrum in Figure-3.

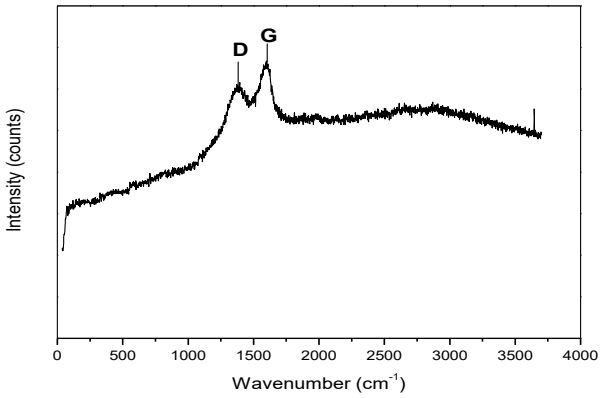

Figure-3. Spectrum of rGO from Raman spectroscopic analysis results.

The spectrum in Figure-3 shows that the G band is located at a wavenumber of 1592 cm^{-1}. This band originates from conjugate bonds or sp^2 carbons produced by vibrations in the plane. Furthermore, the D band at a wavenumber of 1381 cm^{-1} indicates structural defects caused by out-of-plane vibrations (Jagiello *et al*., 2020). The 2D band in the form of a widened peak located at a wavenumber of 2685 cm^{-1} shows a decrease in the rGO structure due to the reduction of oxygen functional groups (Tkachev *et al*., 2012).

The 2D band shows a structure resembling graphene oxide because the matoa leaf extract's reduction process is not optimal. The test with Raman spectroscopy obtained the carbon allotrope's intensity value, indicating material and graphitic defects. The material defect (I_D) and graphitic (I_G) intensity obtained is 305.28 cps and 327.34 cps. The I_D/I_G ratio indicating the size of the structural

defects is calculated to obtain a ratio of 0.93. This ratio increases with the degree of disturbance (Jagiello *et al*., 2020).

Determination of optimum concentration

This stage is the first step in the analysis of adsorption data. The optimum concentration is at the maximum condition absorbed by the adsorbent. The adsorption percentage data at various concentrations are shown in Table 3 and Figure-4.

Table-3. Adsorption percentage with concentration variation on graphite,GO, and rGO.

C_o (ppm)	Adsorption Percentage (%)		
	Graphite	GO	rGO
30	52.73	86.04	95.83
40	41.75	72.06	87.78
50	35.77	62.44	73.91
60	28.30	51.07	61.03
70	24.24	42.96	51.84

Table 3 shows that the adsorption percentage decreases with the optimum percentage of 95.83%. The relationship between concentration variations and adsorbed MB is shown in Figure-4.

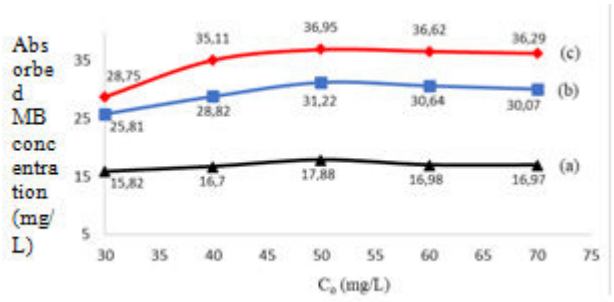

Figure-4. Effect curve of concentration variation on graphite (a), GO (b), and rGO (c).

Figure-4 shows that rGO has better adsorption ability, and the optimum adsorbate concentration is 50 mg/L with an MB of 36.95 mg/L in rGO. The adsorbed MB concentration increases at 30, 40, and 50 mg/L, then decreases at 60 and 70 mg/L. The number of adsorbent molecules causes the decrease at a higher concentration exceeding the available active sites (Nizam *et al*., 2021).

Determination of optimum time

This step is carried out after determining the optimum adsorption concentration. The optimum contact time is determined by the interaction of the adsorbate absorbed at a maximum condition. The adsorption data are shown in Table-4 and Figure-5.

Table-4. Adsorption percentage with time variation on graphite, GO, and rGO

Time (minute)	Adsorption Percentage (%)		
	Graphite	GO	rGO
15	34,64	60,08	64,22
30	35,77	62,44	73,91
45	39,52	70,08	84,81
60	37,72	69,84	84,56
75	38,86	69,10	83,67

Based on Table-4 and Figure-5, the optimum contact time is 45 minutes with an adsorption percentage of 84.81% and adsorbed MB of 42.4 mg/L in rGO. Meanwhile, the increase in concentration occurs at the contact time of 15, 30, and 45 minutes but decreases at 60 and 75 minutes. The decrease is due to the lack of active adsorbent sites available for further adsorption after reaching equilibrium (Jain *et al*., 2016).

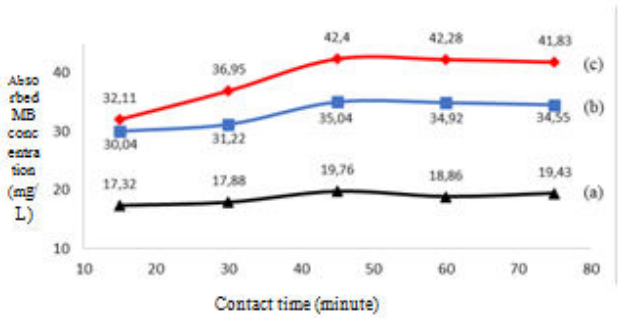

Figure-5. Effect curve of contact time variation on graphite (a), GO (b), and rGO (c).

Determination of optimum adsorbent mass

This step is conducted after determining the optimum adsorption concentration and time. The optimum adsorbent mass is obtained when the amount of adsorbate absorbed by an adsorbent is at the maximum. The adsorption data are shown in Table-5 and Figure-6.

Table-5. Adsorption percentage with a mass variation on graphite, GO, and rGO.

Mass (mg)	Adsorption Percentage (%)		
	Graphite	GO	rGO
5	32.03	53.81	70.33
10	39.52	70.08	84.81
15	56.92	82.94	98.85
20	64.08	93.12	99.48
25	69.51	99.13	99.72

Table-5 and Figure-6 show that the optimum adsorbent mass is 25 mg with an adsorption percentage of 99.72% and adsorbed MB of 49.856 mg/L in rGO. Figure-

9 indicates the increasing adsorbed MB, and the concentration is caused by the larger surface area of the adsorbate binding to the adsorbent (Obuge *et al*., 2014).

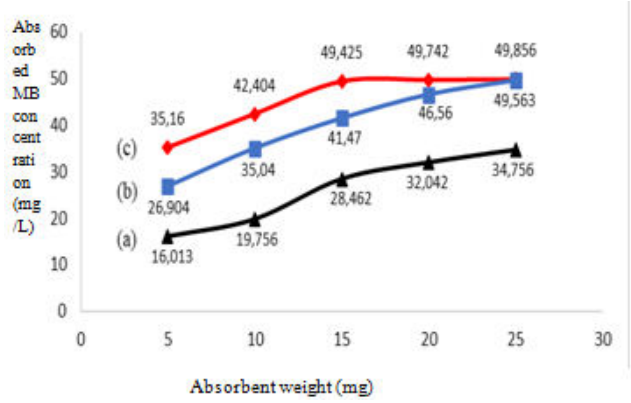

Figure-6. Effect curve of mass variation on graphite (a), GO (b), and rGO (c).

Determination of adsorption isotherm

Equilibrium data for MB adsorption into solid samples are determined using the Langmuir and Freundlich isotherm model (Liu *et al*., 2018). Furthermore, adsorption occurs on the monolayer, and the adsorption sites are homogeneous with the same capacity (Kuang *et al*., 2020). The Freundlich adsorption isotherm is based on the assumption that multi-layer processes occur on heterogeneous solid surfaces (Kuang *et al*., 2020).

Based on Table-6, the correlation coefficient (R^2) obtained is 0.999 in rGO. Therefore, the material more closely follows the Langmuir isotherm model. The maximum concentration of MB adsorption is 54.9 mg/g, indicating a better adsorption ability of rGO. The largest Langmuir constant (K_L) is 0.59 L/mg at rGO, representing the adsorption energy. The large KL value shows a strong interaction between the adsorbate and the adsorbent (Nikman *et al*., 2017).

Table-6. Adsorption isotherm calculation data.

Sample	Langmuir			Freundlich		
	K_L	Q_m	R^2	K_f	1/n	R^2
Graphit	0.07	26.0	0.996	20.9	0.006	0.43
GO	0.20	46.3	0.998	35.6	0.075	0.77
rGO	0.59	54.9	0.999	44.4	0.071	0.79

CONCLUSIONS

a) The synthesis of rGO from OPEFB with matoa leaf extract has not been successfully performed because the mole ratio does not match, and the neutral molecule makes the GO reduction process difficult. Through XRD analysis, the characterization results show an angle 2θ peak of 24.4° with a d-spacing value of 0.365 nm. Furthermore, it reports an absence of functional groups containing oxygen and the relatively decreased intensity of rGO as an FTIR analysis results, and line D at 1381 cm^{-1}, G at 1592 cm^{-1}, and 2D at 2685 cm^{-1} with an I_D/I_G ratio of 0.93 in the Raman analysis.

b) The optimum condition for absorption of methylene blue is a concentration, contact time, and optimum adsorbent mass of 50 ppm, 45 minutes, and 25 mg.

c) The rGO adsorption isotherm follows the Langmuir model with a maximum capacity of 54.945 mg/g.

ACKNOWLEDGMENT

The research/publication of this article was funded by the budget of the Directorate of Research, Technology and Community Service of the Ministry of Education, Culture, Research, and Technology for the fiscal year 2022 through SP DIPA-023.17.1.690523/2022 3rd revision, dated 27 June 2022 and in accordance with SPPK Number: 245/E5/PG.02.00.PT/2022.

REFERENCES

[1] Akhavan O., Bijanzad K. and Mirsepah A. 2014. Synthesis of Graphene from Natural and Industrial Carbonaceous Wastes. RSC Advances. 4(39): 20441-20448.

[2] Chasanah U., Trisunaryanti W., Triyono Oktaviano H. S. and Fatmawati D. A. 2021. The Perfomance of Green Synthesis of Graphene Oxide Prepared by Modified Hummers Method with Oxidation Time Variation. Rasayan Journal of Chemistry. 14(3): 2017-2023.

[3] Grace A. S. and Malar G. S. P. L. 2020. Synthesis and Characterization of Graphene Oxide from Coconut Husk Ash. Oriental Journal of Chemistry. 36(2): 348-352.

[4] Handayani W., Ningrum A. S. and Imawan C. 2020. The Role of pH in Synthesis Silver Nanoparticles Using Pometia pinnata (Matoa) Leaves Extract as Bioreductor. Journal of Physics: Conference Series. 1428 (012021): 1-5.

[5] Hashmi S., Mushtaq A., Ahmed R. and Ali Z. U. 2022. Synthesis and Characterization of Reduced Graphene Oxide from Indegenous Coal: A Non-Burning Solution. International Journal of Membrane Science and Technology. 9(1): 1-12.

[6] Hessein H. A. and Hassan J. J. 2020. Green Synthesis of Reduced Graphene Oxide Using Ascorbic Acid. Iraqi Journal of Science. 61(6): 1313-1319.

[7] Hidayah N. M. S., Liu W. W., Lai C. W., Noriman M. Z., Khe C. S., Hashim U. and Lee H. C. 2017. Comparison on Graphite, Graphene Oxide, and Reduced Graphene Oxide: Synthesis and Characterization. AIP Conference Proceedings. 1892(150002): 1-8.

[8] Jagiello J., Chlanda A., Baran M., Gwiazda M. and Lipinska L. 2020. Synthesis and Characterization of Graphene Oxide & Reduced Graphene Oxide Composites with Inorganic Nanoparticle Biomedical Applications. Nanomaterials. 10(846): 1-18.

[9] Jain N., Dwivedi M. K. and Waskle A. 2016. Adsorption of Methylene Blue Dye from Industrial Effluents Using Coal Fly Ash. International Journal of Advanced Engineering Research and Science. 3(4): 9-16.

[10] Jirickova A., Jankovsky O., Sofer Z. and Sedmidubsky D. 2022. Synthesis and Applications of Graphene Oxide. Materials. 15(920): 1-21.

[11] Joshi S., Siddiqui R., Sharma P., Kumar R., Verma G. and Saini A. 2020. Green Synthesis of Peptide Functionalized Reduced Graphene Oxide (rGO) Nano Bioconjugate with Enhanced Antibacterial Activity. Nature Research Scientific Report. 10(9441): 1-11.

[12] Khan M. I. 2020. Adsorption of Methylene Blue onto Natural Saudi Red Clay: Isotherms, Kinetics and Themodynamics Studies. Materials Research Express. 7(055507). 1-13.

[13] Kuang Y., Zhang X. and Zhou S. 2020. Adsorption of Methylene Blue in Water onto Activated Carbon by Surfactant Modification. Water. 12(587): 1-19.

[14] Kusrini E., Suhrowati A., Usman A., Khalil, M. and Degirmenci V. 2019. Synthesis and Characterization of Graphite Oxide, Graphene Oxide, and Reduced Graphene Oxide from Graphite Waste Using Modified Hummers Method and Zinc as Reducing Agent. International Journal of Technology. 10(6): 1093-1104.

[15] Li C., Zachao Z., Xiaoying J. and Zuliang. 2017. A Facile and Green Preparation of Reduced Graphene Oxide Using Eucalyptus Leaf Extract. Journal of Applied Surface Science. 422(1): 469-474.

[16] Liu Q. X., Zhou Y. R., Wang M., Zang Q., Ji T., Chen T. Y. and Yu D. C. 2019. Adsorption of Methylene Blue from Aqueous Solution onto Viscose-Based Activated Carbon Fiber Felts: Kinetics and Equilibrium Studies. Adsorption Science and Technology. 37(3-4): 312-332.

[17] Magne T. M., Vieira T. O., Alencar L. M. R., Junior F. F. M., Piperni S. G., Carneiro S. V., Fechine L. M. U. D., Freire R. M., Golokhvast K., Metrangolo P., Fechine P. B. A. and Oliveira R. S. 2021. Graphene and Its Deritatives: Understanding the Main Chemical and Medicinal Chemistry Roles for Biomedical Application. Journal of Nanostructure in Chemistry. 1(1): 1-35.

[18] Nikman K. A., Ahmad F., Hassan, M. S., Nikman K. and Ahmad M. A. 2017. Adsorption of Chemical Prepared Cocoa Nibs Based Activated Carbon onto Methylene Blue: Equilibrium and Kinetic Studies. International Journal of Petrochemistry and Research. 1(1): 15-18.

[19] Nizam N. U. M., Hanafiah M. M., Mahmoudi E., Halim A. A., and Mohammad A. W. 2021. The Removal of Anionic and Cationic Dyes from An Aqueous Solution Using Biomass-Based Activated Carbon. Nature Scientific Report. 11(8623): 1-17.

[20] Novoselov K. S., Geim A. K., Morozov S. V., Jiang D., Zhang Y., Dubonos S. P., Grigorieva L. I. and Firsov A. A. 2004. Electric Field Effect in Atomically Thin Carbon Films. Science. 306(5696): 666.

[21] Obuge Macaulay A. and Evbuomwan O. B. 2014. Adsorption of Methylene Blue onto Activated Carbon Impregnated with KOH Using Cocoa Shell. International Journal of Engineering and Technical Research. 2(10): 11-18.

[22] Padzil F. N. M., Lee S. H., Ainun Z. M. A., Lee C. H., and Abdullah L. C. 2020. Potential of Palm Empty Fruit Bunch Resources in Nanocellulose Hydrogel Production for Versatile Applications: A Review. Materials. 13(1245): 1-26.

[23] Parthipan P., Monerah A. A., Al-Ghamdi A. A. and Subramania A. 2021. Eco-Friendly Synthesis Reduced Graphene Oxide as Sustainable Photocatalyst for Removal of Hazardous Organic Dyes. Journal of King Saud University. 1(33): 101438.

[24] Rahayu, D. E., Karnaningroem, N., Altway, A., and Slamet, A. 2021. Utilization of Oil Palm Empty Fruit Bunches Biomass through Slow Pyrolysis Process. IOP Conference Series: Earth and Env. Science. 913(012018): 1-7.

[25] Ranjan P., Agrawal S., Sinha A., Rao T. R., Balakhrishnan J. and Thakur A. D. 2018. A Low-Cost Non-Explosive Synthesis of Graphene Oxide for Scalable Applications. Springer Nature Scientific Reports. 8(12007): 1-14.

[26] Razaq A., Bibi F., Zheng X., Papadakis R. and Jafri S. H. M. 2022. Review of Graphene, Graphene Oxide, Reduce Graphene Oxide Based Flexible Composites: from Fabrication to Applications. Materials. 15(102): 1-17.

[27] Rebitanim N. Z., Azlina W., Ghani W. A. K., Mahmoud D. K., Rebitanim A., Amran M. and Salleh, M. 2012. Adsorption Capacity of Raw Empty Fruit Bunch Biomass onto Methylene Blue Dye in Aqueous Solution. Journal of Purity. 1(1): 45-60.

[28] Sari D. W., Hidayat F. N. and Abdul I. 2021. Efficiency of Land Use in Smallholder Palm Oil Plantations in Indonesia: A Stochastic Frontier Approach. Forest and Society. 5(1): 75-89.

[29] Shao G., Lu Y., Wu F., Yang C., Zeng F. and Wu Q. 2012. Graphene Oxide: The Mechanisms of Oxidation and Exfoliation. Journal of Material Science. 47(10): 4400-4409.

[30] Smith A. T., Lachance A. M., Zeng S., Liu B. and Sun L. 2019. Synthesis, Properties and Application of Graphene Oxide/ Reduced Graphene Oxide and Their Nanocomposites. Nano Materials Science. 1(1): 31-47.

[31] Suma Y., Pasukphun N., and Eaktasang N. 2021. Adsorption of Methylene Blue by Low-Cost Biochar Derived from Elephant Dung. Applied Environmental Research. 43(3): 34-44.

[32] Teow Y. H., Athirah W. N., Hamdan W. M. and Mohammad A. W. 2021. Preparation of Palm Oil Industry's Biomass-Based Graphene Composite for The Adsorptive Removal of Methylene Blue. Adsorption Science and Technology. 1(1): 1-11.

[33] Thoe J. M. L., Surugau N. and Chong H. L. H. 2019. Application of Oil Palm Empty Fruit Bunch as Adsorbent: A Review. Transactions on Science and Technology. 6(1): 9-26.

[34] Tkachev S. V., Buslaeva E. Y., Naumkin Kotova, S. L., Laura I. V, and Guvin S. P. 2012. Reduced Graphene Oxide. Inorganic Materials. 48(8): 796-802.

[35] Wang Z., Gao M., Li X., Ning J., Zhou Z. and Li G. 2020. Efficient Adsorption of Methylene Blue from Aqueous Solution by Graphene Oxide Modified Persimmon Tannins. Materials Science and Engineering C. 108(110196): 1-9.

[36] Widiatmoko P., Sukmana I. F., Nurdin I., Prakoso T. and Devianto H. 2019. Increasing Yield of Graphene Synthesis from Oil Palm Empty Fruit Bunch via Two-Stage Pyrolysis. International Journal of Technology. 1(1): 612-620.

[37] Yang H., Li H., Zhai J., Sun L. and Yu H. 2014. Simple Synthetic of Graphene Oxide Using Ultrasonic from Expanded Graphite. Industrial and Engineering Chemistry Research. 1(1): 1-6.

[38] Yang Y., Wang Z. and Zheng S. 2022. Secondary Exfoliation of Electrolytic Graphene Oxide by Ultrasound Assisted Microwave Technique. Nano materials. 12(68): 1-9.